Peli1 negatively regulates T-cell activation and prevents autoimmunity

Mikyoung Chang[1,*], Wei Jin[1,5,*], Jae-Hoon Chang[1], Yi-chuan Xiao[1], George Brittain[1], Jiayi Yu[1], Xiaofei Zhou[1], Yi-Hong Wang[1], Xuhong Cheng[1], Pingwei Li[4], Brian A Rabinovich[2], Patrick Hwu[3], and Shao-Cong Sun[1]

[1]Department of Immunology, [2]Immunology Laboratory of Physician Scientists, [3]Department of Melanoma Medical Oncology, The University of Texas MD Anderson Cancer Center, 7455 Fannin Street, Box 902, Houston TX 77030. [4]Department of Biochemistry and Biophysics, 2128 TAMU, Texas A&M University, College Station, TX 77843-2128.

[5]Present address: Howard Hughes Medical Institute and Immunology Program, Memorial Sloan-Kettering Cancer Center, New York, NY 10065, USA.

[*]These authors contributed equally to this work

Correspondence should be addressed to S.-C.S. (ssun@mdanderson.org)

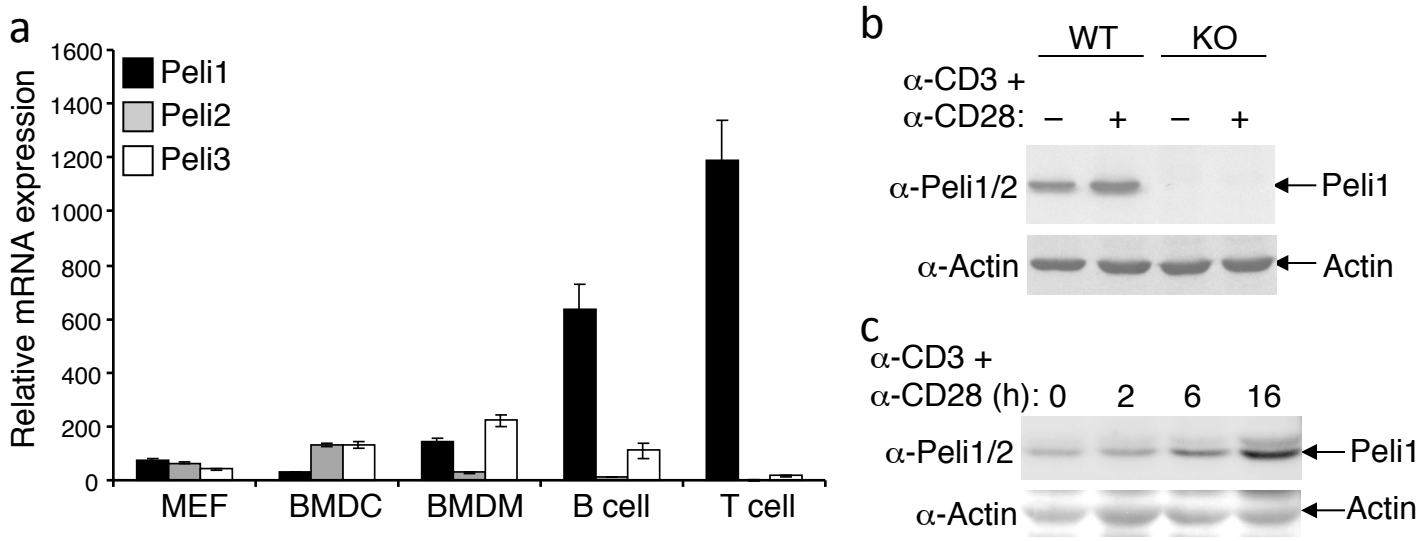

Supplementary Figure 1. Abundant expression and inducibility of Peli1 in T cells. (**a**) Real-time RT-PCR was performed using RNA isolated from murine embryonic fibroblast (MEF), bone marrow-derived dendritic cells (BMDC), bone marrow-derived macrophages (BMDM), spleen B cells, and spleen T cells. The relative mRNA expression was calculated as fold based on the lowest value (Peli2 expression in T cells). (**b**) Spleen T cells derived from wild-type (WT) or *Peli1*$^{-/-}$ (KO) mice were either untreated (–) or stimulated for 16 hr with anti-CD3 (1 μg/ml) plus anti-CD28 (1 μg/ml). Total cell lysates were subjected to immunoblotting assays using an antibody that recognizes both Peli1 and Peli2 (anti-Peli1/2) or the anti-actin antibody. (**c**) Spleen T cells from wild-type mice were stimulated with anti-CD3 plus anti-CD28 for the indicated times and then subjected to IB analysis using whole-cell lysates. Reduced amounts of cell lysates were loaded to better visualize the inducible expression of Peli1.

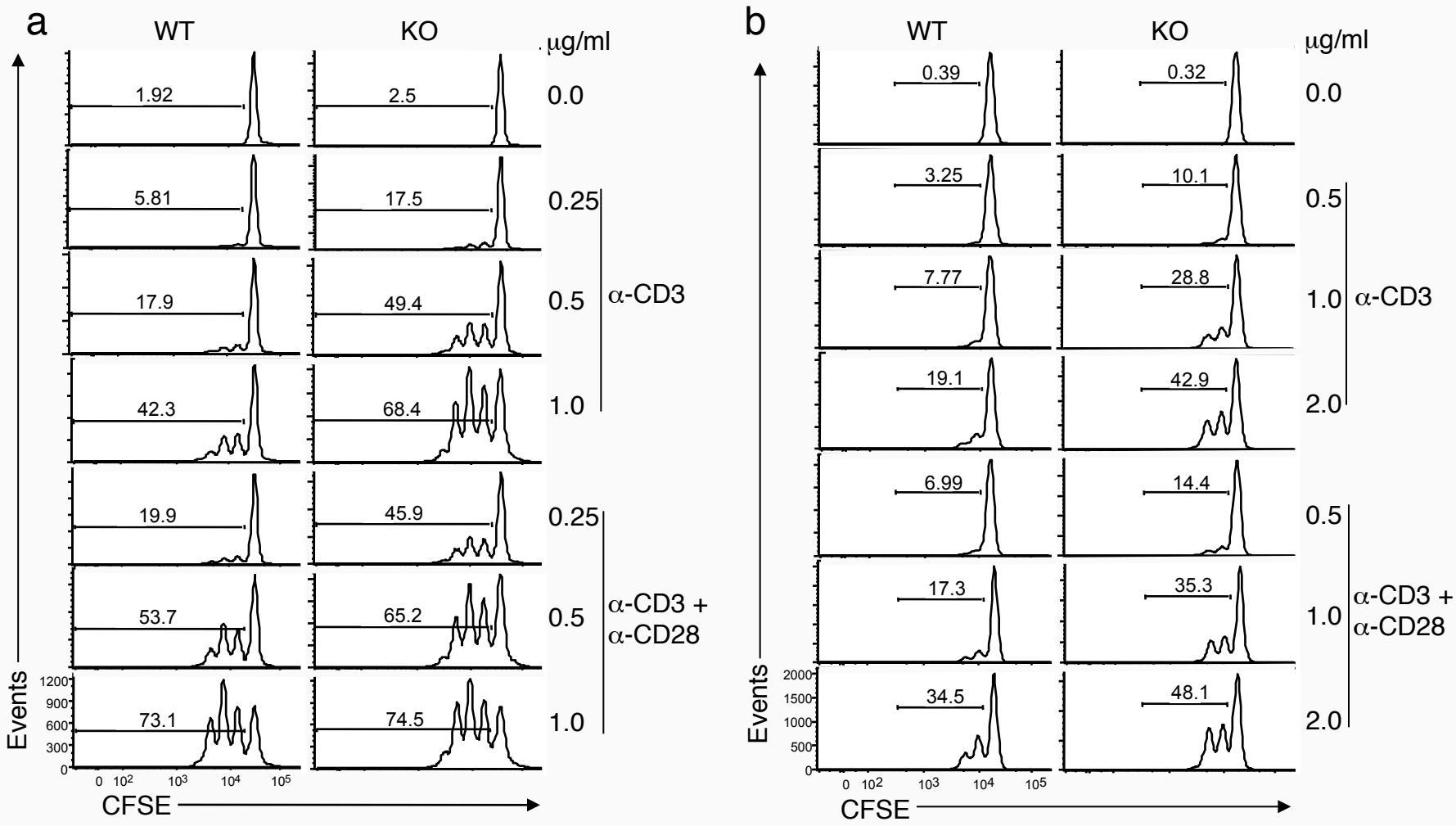

Supplementary Figure 2. Hyperproliferative response of Peli1-deficient CD8 T cells to TCR stimulation. Total (**a**) and naïve (**b**) CD8 T cells, derived from wild-type (WT) or *Peli1*$^{-/-}$ (KO) mice, were labeled with CFSE and stimulated for 48 hr with the indicated doses of pate-bound anti-CD3 either in the absence or the presence of anti-CD28 (same doses as anti-CD3). Cell proliferation was measured by flow cytometry and determined based on CFSE dilution. The percentage of dividing cells is indicated. Data are representative of three independent experiments.

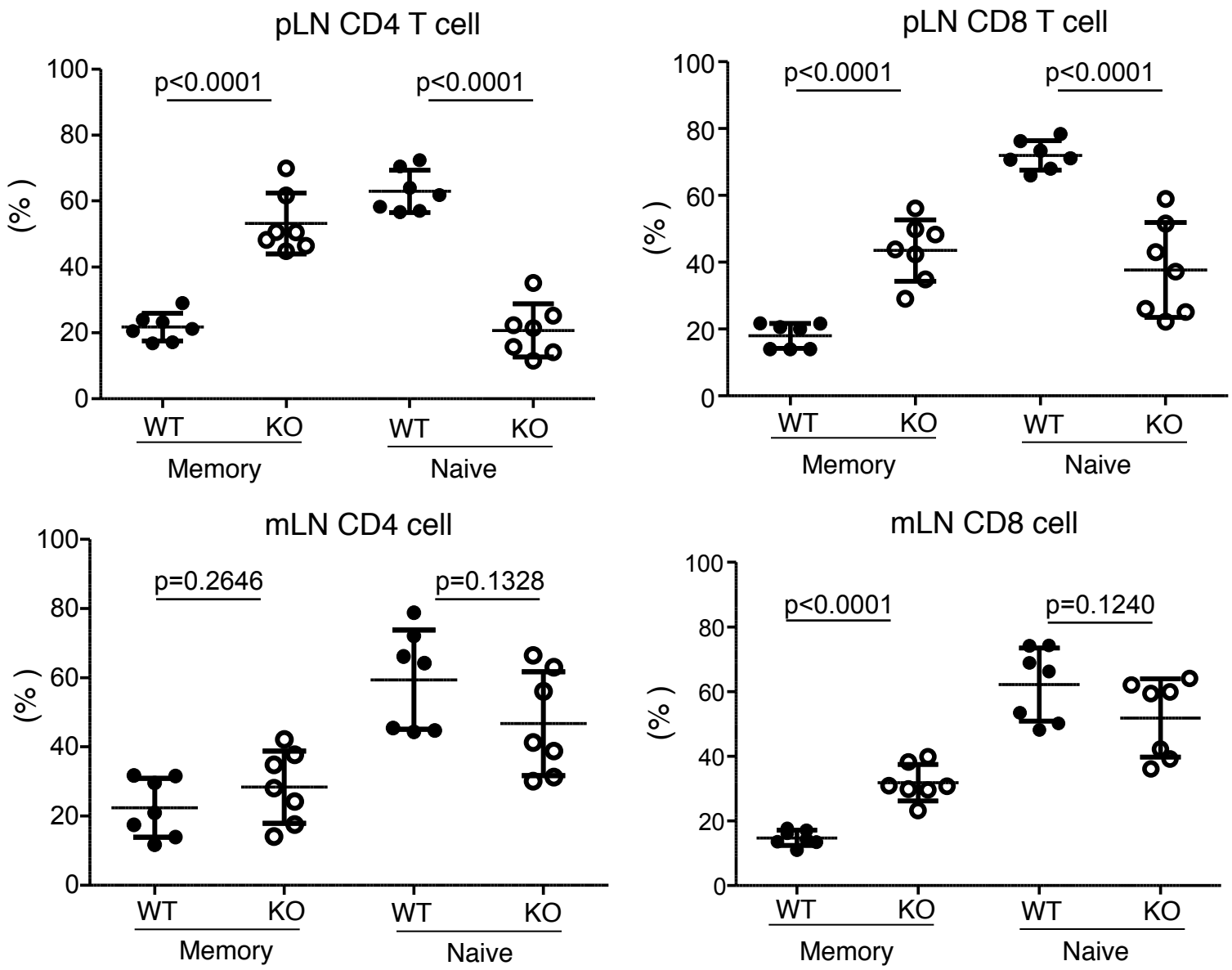

Supplementary Figure 3. Peli1 knockout mice have increased frequency of memory T cells in peripheral lymph nodes. CD4 and CD8 memory ($CD44^{hi}CD62^{lo}$) and naïve ($CD44^{lo}CD62^{hi}$) T cells were measured by flow cytometry using cells isolated from peripheral lymph nodes (pLN) or messentary lymph nodes (mLN) of age-matched wild-type (WT) and *Peli1*$^{-/-}$ (KO) mice (6 month or older). Frequency among total CD4 or CD8 T cells is presented. Multiple mice were analyzed (each circle represents a mouse) to obtain statistical value.

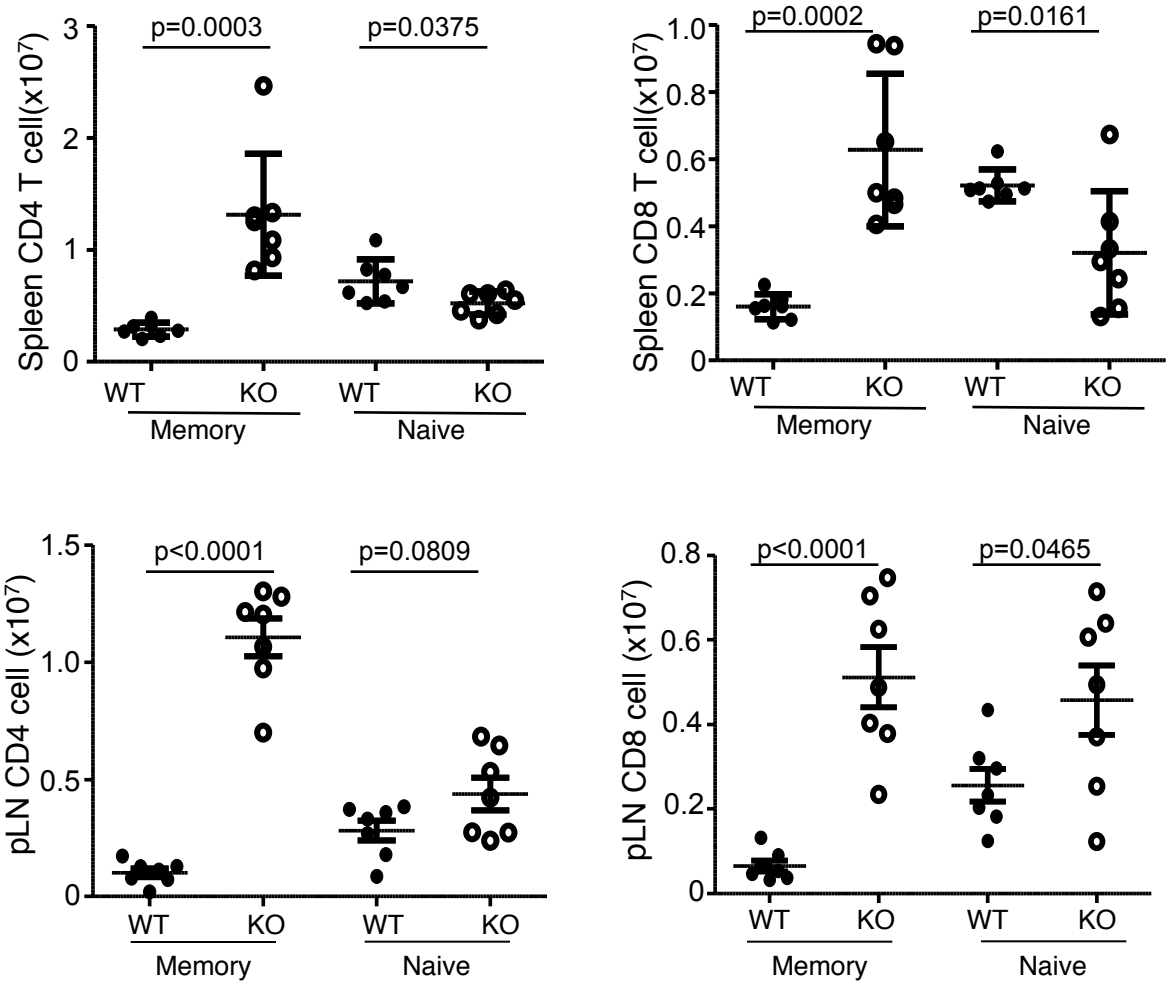

Supplementary Figure 4. Peli1 knockout mice display increased numbers of memory T cells in the spleen and peripheral lymph nodes. CD4 and CD8 memory ($CD44^{hi}CD62^{lo}$) and naïve ($CD44^{lo}CD62^{hi}$) T cells were measured by flow cytometry using cells isolated from the spleen and peripheral lymph nodes (pLN) of age-matched wild-type (WT) and *Peli1*$^{-/-}$ (KO) mice (6 month or older). Absolute cell numbers were calculated based on total cell numbers of the corresponding lymphoid organs. Multiple mice were analyzed (each circle represents a mouse) to obtain statistical value.

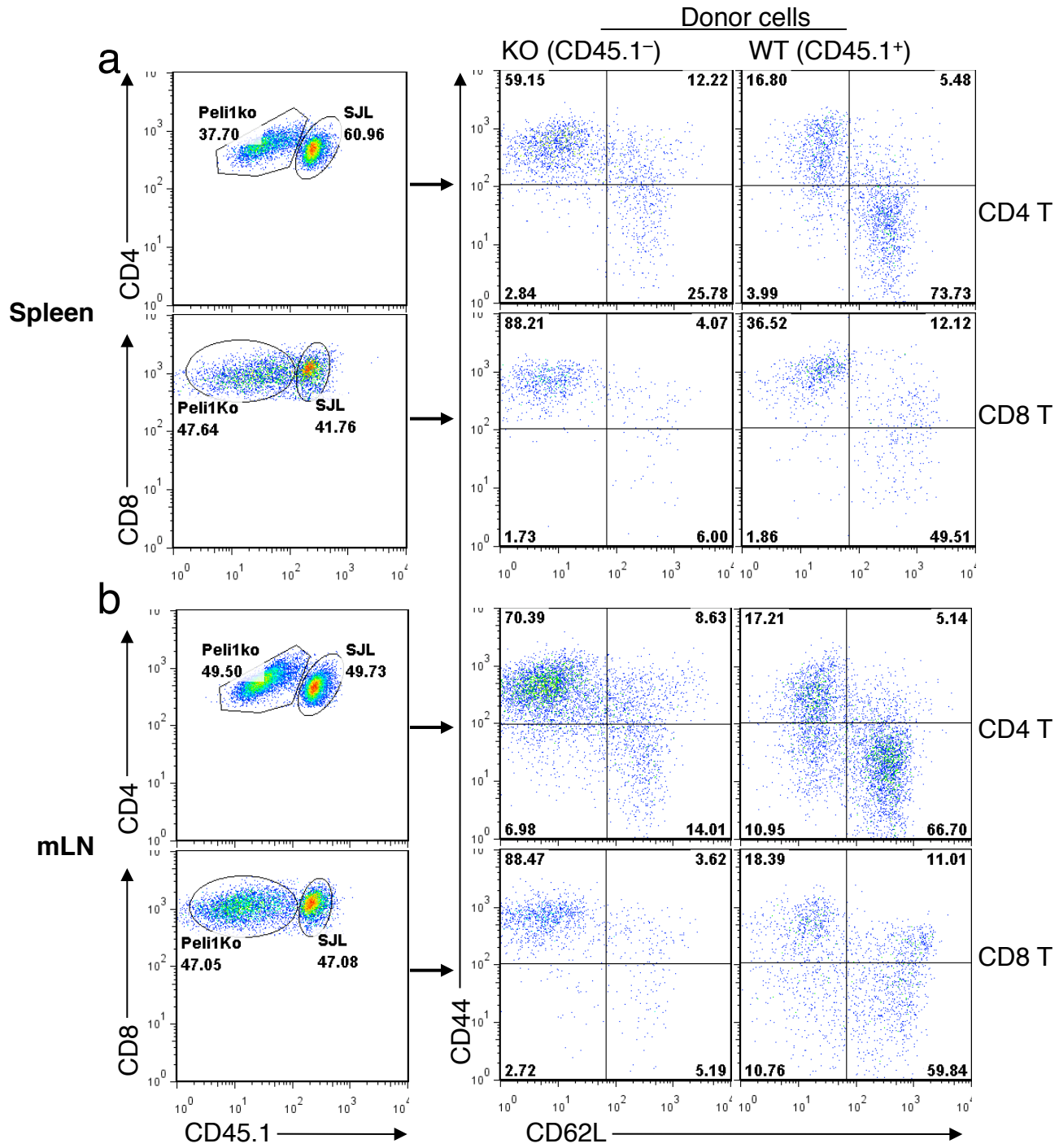

Supplementary Figure 5. T-cell intrinsic function of Peli1 in the regulation of T-cell activation. Bone marrow cells from *Peli1*$^{-/-}$ (KO) (CD45.1^{-}) and wild-type (WT) B6.SJL (CD45.1^{+}) mice were mixed in 1:1 ratio and adoptively transferred into γ-irradiated Rag1$^{-/-}$ mice. After 10 weeks, recipient mice were sacrificed for flow cytometry analyses using spleen (**a**) and mesentery lymph node (**b**) cells. Left panels show the frequency of CD45.1^{-} (KO) and CD45.1^{+} (WT, SJL) CD4 and CD8 T cells. The frequency of memory and naïve T cells within the KO and WT (SJL) CD4 and CD8 T-cell populations were determined based on CD44 and CD62L markers (naïve: CD44^{lo}CD62L^{hi}; memory: CD44^{hi}CD62L^{lo}). Data are representative of four recipients of each group.

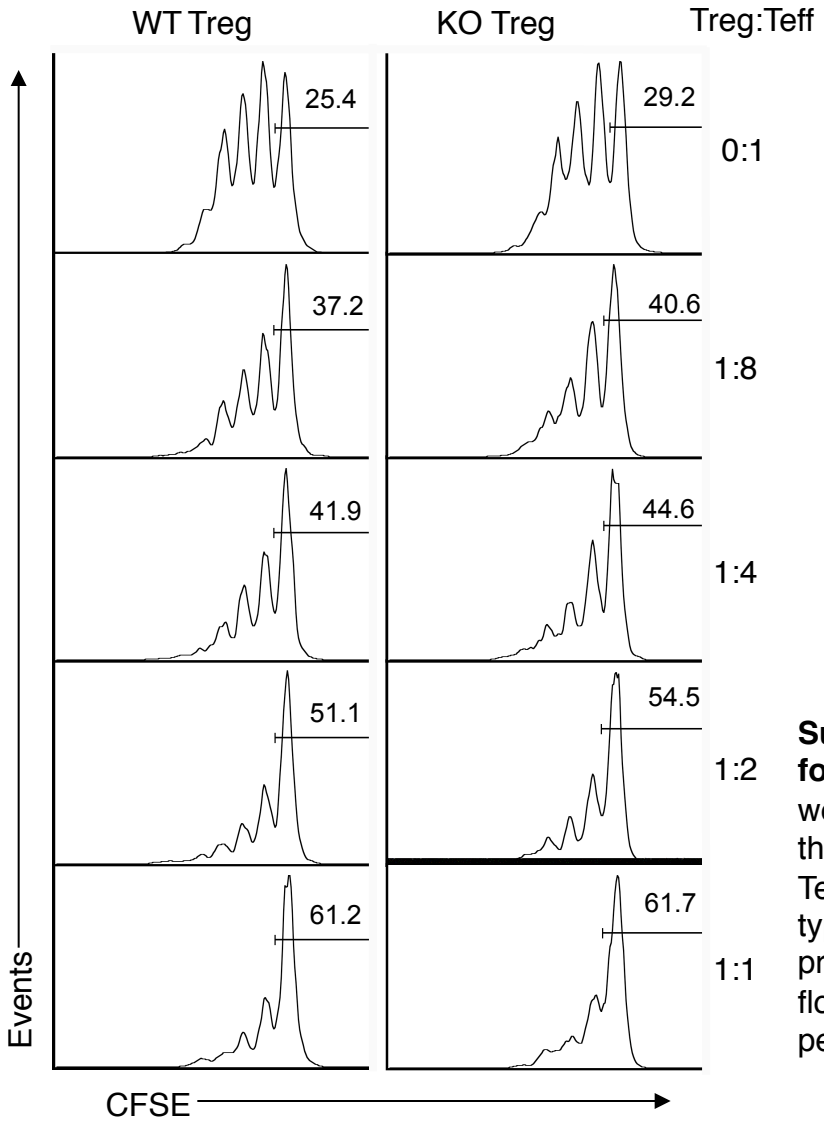

Supplementary Figure 6. Peli1 is dispensable for Treg function. Wildtype naïve CD4 T cells were labeled with CFSE and activated in vitro in the presence of the indicated ratios (Treg-to-Teffector) of Treg cells isolated from either wild-type (WT) or *Peli1*$^{-/-}$ (KO) mice (8 weeks old). The proliferation of effector T cells was analyzed by flow cytometry based on CFSE dilution. The percentage of non-divided cells is indicated.

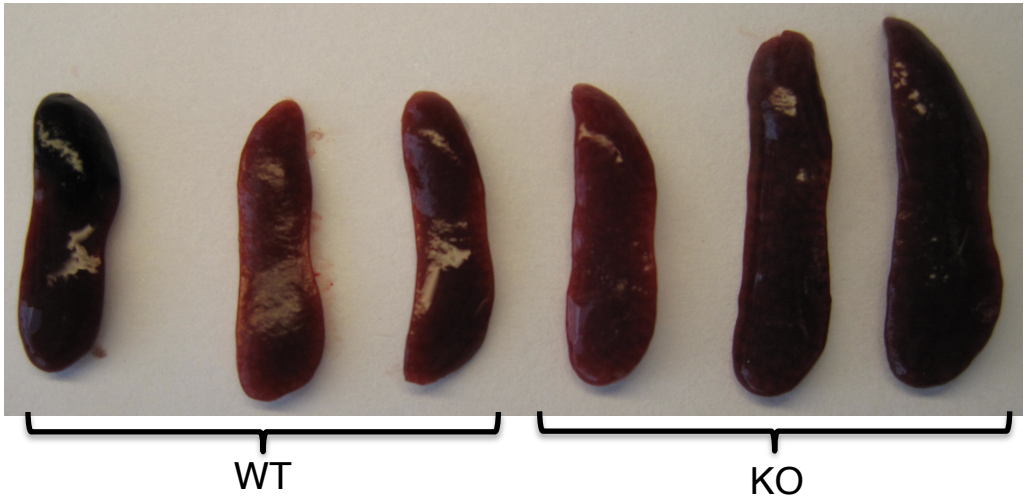

Supplementary Figure 7. Splenomegaly of *Peli1*$^{-/-}$ (KO) mice. Picture of spleens of age-matched wild-type (WT) and KO mice (3 per group; 6 mon old), showing moderate splenomegaly of the KO mice.

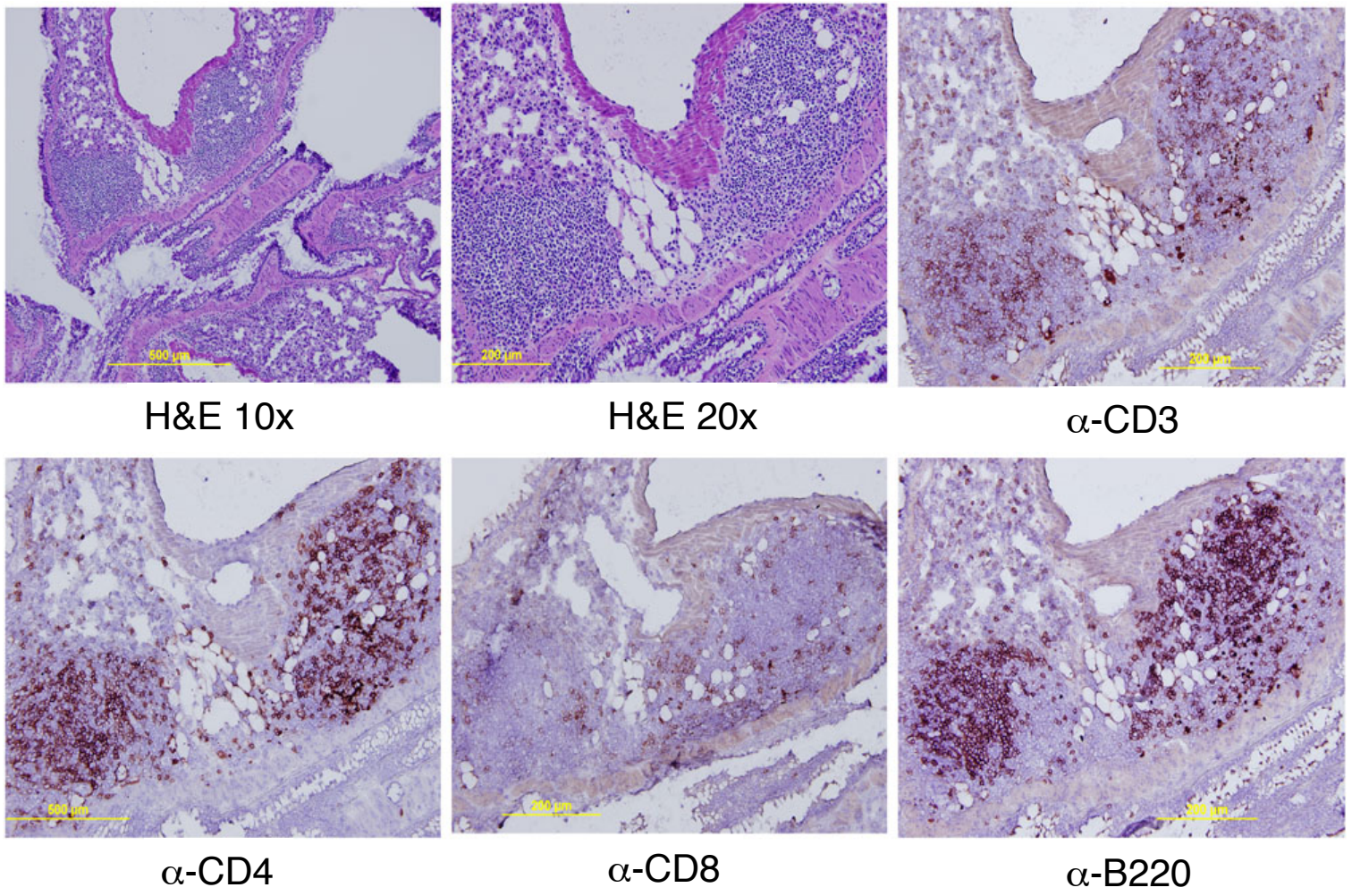

Supplementary Figure 8. Lymphocyte infiltration into the lung of *Peli1*$^{-/-}$ (KO) mice. Lung tissue sections from 6 month old KO mice were subjected to hematoxylin-eosin staining (panels 1 and 2; presented at 10x and 20x of original magnification) or immunohistochemistry using anti-CD3, anti-CD4, anti-CD8, or anti-B220 antibodies (original magnification, 20x). Data are representative of multiple mice.

a

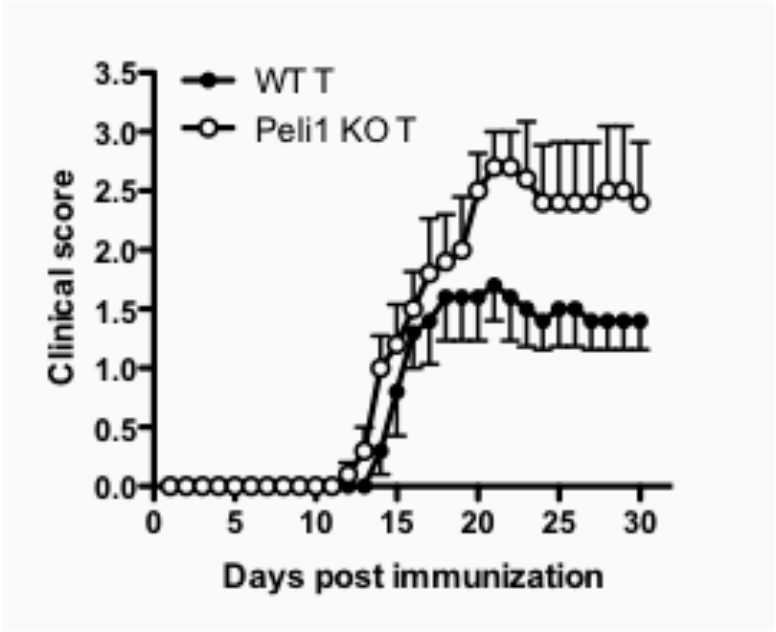

b

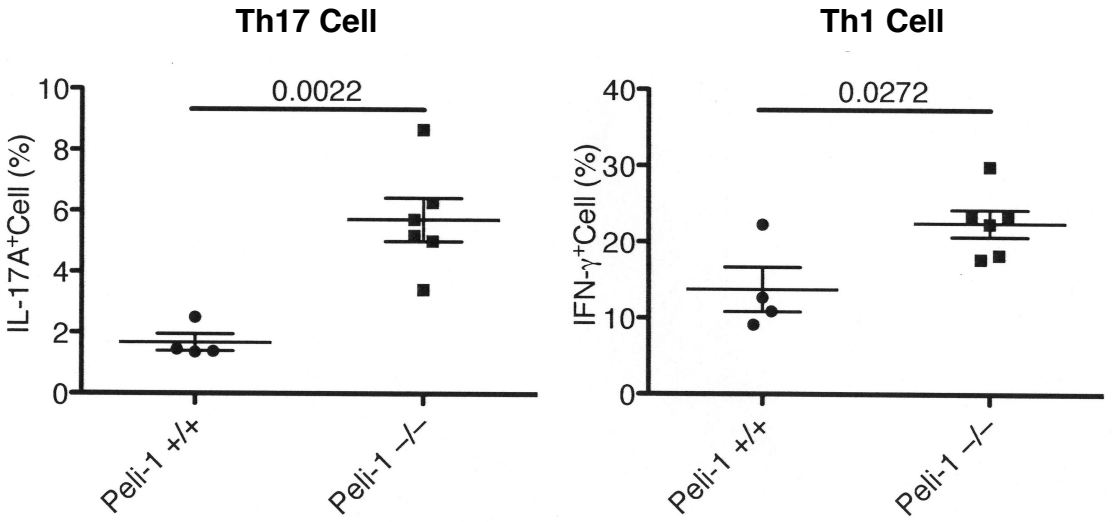

Supplementary Figure 9. Induction of EAE autoimmunity property of *Peli1*-deficient T cells. T cells of wild-type (WT) and *Peli1*$^{-/-}$ (KO) mice (8 weeks old) were adoptively transferred into *Rag1*$^{-/-}$ mice. After 16 hr of adoptive transfer, the recipient mice were immunized for EAE induction as described in Methods. (**a**) EAE disease scores showing more severe diseases in recipients of the *Peli1* KO T cells. (**b**) Immunized recipients of *WT* or *KO* T cells were sacrificed on day 16 after immunization. Spleen T cells were subjected to intracellular cytokine staining to determine the frequency of Th17 and Th1 cells (among CD4 T cells) based on expression of IL-17A and IFN-γ, respectively.

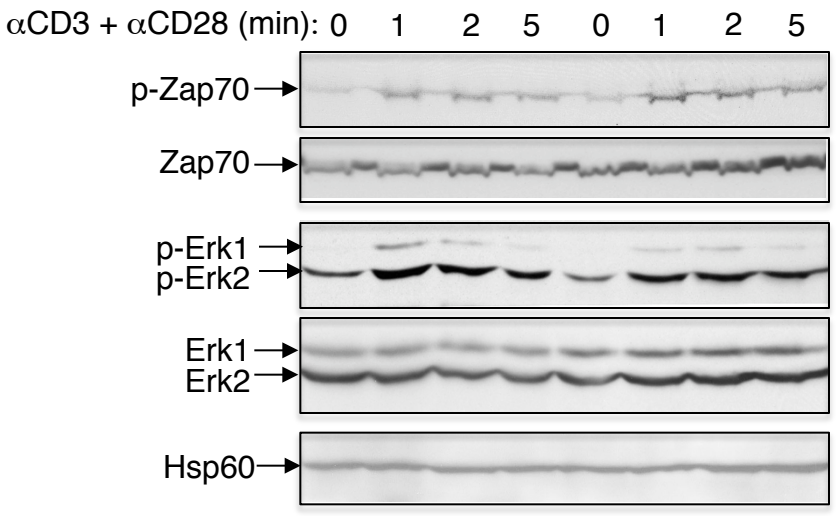

Supplementary Figure 10. Peli1 deficiency has no effect on proximal TCR signaling. T cells were incubated with anti-CD3 plus anti-CD28 on ice and then stimulated with an anti-Ig secondary antibody for the indicated times. Phosphorylation of Zap70 and Erk was analyzed by IB using their phospho-specific antibodies. The membranes were then stripped and reprobed with corresponding regular antibodies.

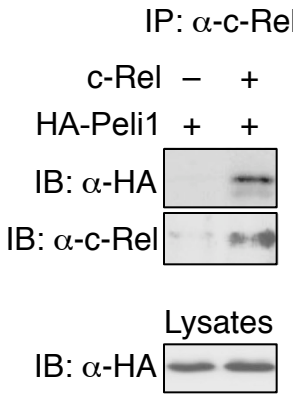

Supplementary Figure 11. Physical interaction between Peli1 and c-Rel. 293 cells were transfected with HA-Peli1 either in the presence (+) or absence (–) of c-Rel. Whole-cell lysates were subjected to immunoprecipitation (IP) with anti-c-Rel followed by detecting the precipitated c-Rel and co-precipitated HA-Peli1 by IB (upper two panels). The lysates were also subjected to direct IB to examine HA-Peli1 expression level (bottom panel).

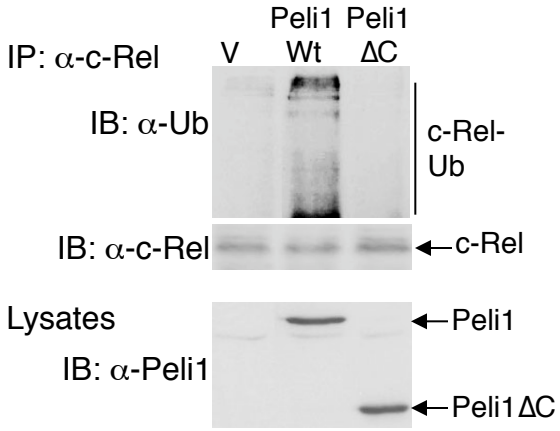

Supplementary Figure 12. Peli1 overexpression in EL4 T cells induces c-Rel ubiquitination. EL4 cells were infected with retroviral vector pRV100G or the same vector encoding wild-type (Wt) Peli1 or a Peli1 mutant lacking the C-terminal RING domain (ΔC). 72 hr after infection, the infected cells were enriched by flow cytometric sorting based on GFP expression (the vector encodes IRES-GFP). The cells were incubated with MG132 (25 μM) for 2 hr, and whole-cell lysates were subjected to c-Rel IP followed by detecting ubiquitinated c-Rel and c-Rel by IB. Exogenous Peli1 and Peli1ΔC were analyzed by IB using anti-Peli1.

T-cell adoptive transfer and EAE induction. Purified T cells were transferred i.v. into *Rag1*$^{-/-}$ mice (20 x 10^6 cells/recipient mouse). After 16 h, EAE was induced essentially as previously described [47]. Clinical symptoms were scored based on a standard method: 0, no clinical signs; 0.5, partially limp tail; 1, limp tail; 2, loss in coordinated movement and hind-limb paresis; 2.5, paralysis of one hind limb; 3, paralysis of both hind-limbs; 3.5, hind-limb paralysis and weakness in forelimbs; 4, paralysis of hind-limbs and forelimbs; 5, moribund or death.

Peli1 knockdown and overexpression in EL4 cells. Murine EL4 T cells were infected with lentiviruses carrying either pLKO.1 or pLKO.1-*Peli1* shRNA. After 48 h, the infected cells were enriched by selection using puromycin (2.0 μg/ml) for 5 days, and the bulk of the infected cells were used in experiments. To produce the lentiviral particles, the pLKO.1 vectors were transfected into HEK293 cells (using calcium method) along with packing vectors psPAX2 and pMD2 (provided by Dr. Xiaofeng Qin). For Peli1 overexpression, pRV100G retroviruses encoding Peli1 or Peli1ΔC were transduced into EL4 cells. 72 hr after infection, the infected cells were enriched by flow cytometric sorting based on GFP expression (the vector encodes IRES-GFP) and used in experiments.

EMSA. Nuclear extracts were prepared from T cells and subjected to EMSA using ^{32}P-radiolabeled oligonucleotide probes for NF-κB (CAACGGCAGGGGAATTCCCCTCTCCTT), AP-1 (GATCTAGTGATGAGTCAGCCG), or the constitutive transcription factor NF-Y

(AAGAGATTAACCAATCACGTACGGTCT). Antibody supershift assays were performed by adding specific antibodies or control Ig to the EMSA reaction.

Real-time quantitative RT-PCR. Total RNA was isolated using TRI reagent (Molecular Research Center, Inc.) and subjected to cDNA synthesis using RNase H-reverse transcriptase (Invitrogen) and oligo (dT) primers. Real-time quantitative PCR was performed in triplicates, using iCycler Sequence Detection System (Bio-Rad) and iQ™ SYBR Green Supermix (Bio-Rad). The expression of individual genes was calculated by a standard curve method and normalized to the expression of GAPDH. The gene-specific primer sets were (all for mouse genes): *Peli1*, 5'-CCTTGTCCATGTAAGTTTCTC-3' and 5'-CAGAGTTCAGAAGTCTGGAACT-3'; *Peli2*, 5-CACTCACGGTGGGAATTCAGAC-3' and 5'-GGAGCTATCACCTATGCTCACC-3'; *Peli3*, 5'-GCATGTGGGACTCTGCCTGCT-3' and 5'-GATCAAGATCTCAGTGACCCTC-3'; GAPDH, 5'-CTCATGACCACAGTCCATGCCATC-3' and 5'-CTGCTTCACCACCTTCTTGATGTC-3'.